Naturally occurring monoepoxides of eicosapentaenoic acid and docosahexaenoic acid are bioactive antihyperalgesic lipids[S]

Christophe Morisseau,[1,*] Bora Inceoglu,[1,*] Kara Schmelzer,[*] Hsing-Ju Tsai,[*] Steven L. Jinks,[†] Christine M. Hegedus,[*] and Bruce D. Hammock[2,*]

Department of Entomology and Cancer Center,[*] and Anesthesiology and Pain Medicine,[†] School of Medicine, University of California, Davis, CA 95616

Abstract **Beneficial physiological effects of long-chain n-3 polyunsaturated fatty acids are widely accepted but the mechanism(s) by which these fatty acids act remains unclear. Herein, we report the presence, distribution, and regulation of the levels of n-3 epoxy-fatty acids by soluble epoxide hydrolase (sEH) and a direct antinociceptive role of n-3 epoxy-fatty acids, specifically those originating from docosahexaenoic acid (DHA). The monoepoxides of the C18:1 to C22:6 fatty acids in both the n-6 and n-3 series were prepared and the individual regioisomers purified. The kinetic constants of the hydrolysis of the pure regioisomers by sEH were measured. Surprisingly, the best substrates are the mid-chain DHA epoxides. We also demonstrate that the DHA epoxides are present in considerable amounts in the rat central nervous system. Furthermore, using an animal model of pain associated with inflammation, we show that DHA epoxides, but neither the parent fatty acid nor the corresponding diols, selectively modulate nociceptive pathophysiology. Our findings support an important function of epoxy-fatty acids in the n-3 series in modulating nociceptive signaling. Consequently, the DHA and eicosapentaenoic acid epoxides may be responsible for some of the beneficial effects associated with dietary n-3 fatty acid intake.**—Morisseau, C., B. Inceoglu, K. Schmelzer, H-J. Tsai, S. L. Jinks, C. M. Hegedus, and B. D. Hammock. **Naturally occurring monoepoxides of eicosapentaenoic acid and docosahexaenoic acid are bioactive antihyperalgesic lipids.** ***J. Lipid Res.*** **2010.** 51: **3481–3490.**

Supplementary key words soluble epoxide hydrolase • central nervous system • pain

A number of beneficial physiological effects have been attributed to dietary n-3 fatty acids including decreasing the risk of cardiovascular diseases, diabetes, inflammation, and pain, although the mechanism(s) by which these fatty acids act is debated (1–3). The two major n-3 polyunsaturated fatty acids (PUFAs), eicosapentaenoic acid (EPA, 20:5 n-3) and docosahexaenoic acid (DHA, 22:6 n-3), are known to compete with arachidonic (ARA, 20:4 n-6) or linoleic acids (LNA, 18:2 n-6) for metabolism by cyclooxygenases (COXs), lipoxygenases (LOXs), and the cytochrome P450 (CYP) enzymes (4–6). This is thought to modulate the production and the bioactivity of prostanoids, leukotrienes, and epoxyeicosanoids (7–10). Alternatively, essential n-3 fatty acids EPA and DHA are also precursors to potent lipid mediators such as resolvins and protectins (11). These new classes of mediators were first proposed to be produced by aspirin acetylated COX and more recently by LOX enzymes (12). Both resolvins and protectins are thought to have lipoxygenase generated epoxygenated intermediates in their biosynthetic pathways (4). Here we investigated the occurrence, metabolism, and biological activity of another class of bioactive lipids, the epoxygenase metabolites of DHA and EPA.

This work was partially funded by National Institute of Environmental Health Sciences grants ES02710 and ES013933, NIEHS Superfund Basic Research Program grant P42 ES04699, and NIGMS grant GM078167. B.D.H. is a George and Judy Marcus Senior Fellow of the American Asthma Foundation.

Manuscript received 5 February 2010 and in revised form 23 July 2010.

Published, JLR Papers in Press, July 27, 2010
DOI 10.1194/jlr.M006007

Abbreviations: ARA, arachidonic acid; BHT, butylated hydroxytoluene; BK_{Ca}, big conductance calcium-activated potassium channel; CNS, central nervous system; COX, cyclooxygenase; CYP, cytochrome P450; DHA, docosahexaenoic acid; DiHN, dihydroxynonadecanoic acid; DiHHep, dihydroxyheptadecanoic acid; DiHET, dihydroxyeicosatrienoic acid; DiHOME, dihydroxyoctadecenoic acid; DP, declustering potential; EET, epoxyeicosatrienoic acid; EPA, eicosapentaenoic acid; EpDPE, epoxydocosapentaenoic acid; EpETE, epoxyeicosatetraenoic acid; EpOME, epoxyoctadecenoic acid; HPETE, hydroperoxideicosatetraenoic acid; HETE, hydroxyeicosatetraenoic acid; HODE, hydroxyoctadecadienoic acid; sEH, soluble epoxide hydrolase; SSTD, surrogate standard; LNA, linoleic acid; LOQ, limit of quantification; LOX, lipoxygenase; MRM, multiple reaction-monitoring; SPE, solid phase extraction; TPP, triphenylphosphine.

[1] These authors contributed equally to this work.
[2] To whom correspondence should be addressed.
e-mail: bdhammock@ucdavis.edu

[S] The online version of this article (available at http://www.jlr.org) contains supplementary data in the form of materials and methods, references, and one table.

CYP enzymes, CYP2J and CYP2C in particular, produce a number of bioactive epoxy-fatty acids (10, 13). Hepatic and renal cytochrome P-450 epoxygenases react equally well with EPA, DHA, and ARA to yield, respectively, multiple epoxyeicosatetraenoic (EpETE), epoxydocosapentaenoic (EpDPE), and epoxyeicosatrienoic (EET) acid regioisomers (5, 13–17). In many cases, the n-3 epoxy-fatty acids demonstrate a similar breadth of activities to the corresponding n-6 fatty acid metabolites although exceptions are likely to exist. EpDPE and EpETE, much like the EET, activate big conductance calcium-activated potassium channels (BK_{Ca}), which can lead to hyperpolarization, thus relaxation of vascular smooth muscle cells (18–20). The antihypertensive, antithrombotic, and anti-atherosclerotic properties of EpDPE and EpETE have been demonstrated in multiple rat models (21–23). Furthermore, in vitro, the EETs, EpDPE, and EpETE inhibit platelet aggregation at concentrations below those affecting thromboxane synthesis (24), suggesting that these natural oxiranes have strong, selective, and possibly specific bioactivities.

In parallel to their biosynthesis by CYP enzymes, the degradation of n-3 epoxy-fatty acids could potentially be mediated by the soluble epoxide hydrolase (sEH; epxh2). The sEH is the primary mammalian enzyme that degrades n-6 fatty acid epoxides to their corresponding vicinal diols (25). In fact, the bioactivity of the EETs is strongly regulated by their catabolism by sEH (25). In vivo, inhibition of sEH has been demonstrated to stabilize EETs and presumably other lipid epoxides to lead to diverse biological activities including antihyperalgesia, antihypertension, and anti-inflammation in animal models. Inhibition of sEH is being considered as a potential therapeutic approach for hypertension, vascular inflammation, and pain (10, 13, 26, 27). Here, we tested the hypothesis that EpDPE and EpETE are substrates for sEH, and that they possess parallel biological activity with EET in reducing pain associated with inflammation. A sensitive analytical method described herein for simultaneous detection of the epoxide and diol metabolites from tissue extracts enabled us to support these hypotheses.

MATERIALS AND METHODS

Chemicals

Unsaturated lipids were purchased from NuChek Prep (Elysian, MN). The 11(12)-EET*d8 was purchased from Cayman Chemical (Ann Arbor, MI). HPLC grade hexane, ethyl acetate, and glacial acetic acid were purchased from Fisher Scientific (Pittsburgh, PA). Acetonitrile and methanol were purchased from EM Science (Gibbstown, NJ) and were used for all reverse-phase HPLC analyses. All other chemical reagents were purchased from either Sigma (St. Louis, MO) or Aldrich Chemical Co. (Milwaukee, WI) unless indicated.

Oxylipin preparation and analysis

EpETE and EpDPE regioisomers were generated by reacting the methyl ester of EPA and DHA receptively with *meta*-chloroperbenzoic acid (*m*CPBA) as described (15). Epoxy and diol lipids were purified on a Gilson (model 302) HPLC (Gilson, Middleton, WI) with a differential refractometer (model R401) detector (Waters, Milford, MA). The oxylipids were stored under nitrogen at −80°C until use. Details of this method are given in the supplemental data. An LC/MS/MS method, similar to the one used for EET (28), was developed and optimized to analyze and quantify these novel oxylipins.

LC/MS/MS instrumentation

All HPLC/MS analyses were performed with a Waters ULPC separation module equipped with a 2.0 × 150mm, 5μm Luna C18 column (Phenomenex, Torrence, CA) held at 40°C. The sample chamber was held at 10°C (28). The HPLC was interfaced to the electrospray ionization probe of a Quattro Ultima tandem-quadrupole mass spectrometer (Waters). Solvent flow rates were fixed at 350 μl/min with a cone gas flow of 125 l/h, desolvation gas flow of 650 l/h, a source temperature of 125°C, and a desolvation temperature of 400°C. Electrospray ionization was accomplished in the negative mode with a capillary voltage fixed at 3.0 kV. For MS/MS experiments, argon was used as the collision gas at a pressure of 2.3×10^3 Torr while quadrupole mass resolution settings were fixed at 12.0 (i.e., 1.5 Da resolution). The photo multiplier voltage was 650 V. Optimal cone voltage and collision voltages were established experimentally.

Optimization of MS/MS parameters

To maximize analytical sensitivity using multi-reaction monitoring, we optimized the declustering potential (DP) needed to produce the molecular ion and the collision energy (CE) to maximize characteristic fragmentation ion abundance (28). First, the intensity of the deprotonated molecular ion was evaluated at DP between −50 and −100V. Epoxides showed maximal ionization with a cone voltage of −65 V (supplementary Table I). The ionization of most of the diols was also maximal for a DP of −65 V, except for α12,13-, α15,16 and γ12,13-diHODe that required a DP of −80 V for optimal ionization. Then at optimal DP values, collision-induced dissociation was optimized to maximize the transition ion abundance. For each analyte, pseudo molecular ion was isolated in the first quadrupole and accelerated into the collision cell gas, leading to collision-induced dissociation of the ion. The composition and intensity of the ions produced during this process are a function of the inherent molecular stability and the energies applied. CEs were increased from −10 V to −30 V. As observed before for linoleate and arachidonate epoxides and diols (28), the most characteristics daughter ion for each analyte was the one resulting from breaking the epoxide ring or the bond between the two alcohols. The optimized CE and characteristic transition ions for each target analyte is displayed in supplementary Table I.

Surrogate internal standards and calibration curves

Surrogate standards [11,12-EET-d_8, 10,11-dihydroxynondecanoic acid (10,11-DiHN) and 10(11)-epoxyheptadecanoid acid (10,11-EpHep)] were added to samples before extraction. For quantification, the analytes were linked to their corresponding surrogates and the correlation between relative response factors. As a control for potential epoxide hydrolysis, 10,11-dihydroxyheptadecanoid acid (10,11-DiHHep), the corresponding diol of 10(11)-EpHep, was also quantified. The internal standard, 1-cyclohexyl-dodecanoic acid urea (CDAU), was added at the last step before analysis to account for changes in volume and instrument variability while quantifying surrogate recoveries. CDAU, 10(11)EpHep, 10,11DHHep, and 10,11-DiHN were synthesized previously (28, 29). Seven independent calibration solutions [from 5 to 1,000 fmol/μL (nM)] containing 1 pmol/μL of each internal standard were prepared in acetonitrile. These standards

contained all EpOME, EET, EpETE, EpDPE, DiHOME, DHET, DiHETE, and DiHDPE isomers.

Determining accuracy and precision

Excellent linearity ($r^2 > 0.999$) was observed for all analytes over the extended concentration range tested (from 5 to 1,000 fmol/μl). This results in a limit of quantification of about 1 nM for each analyte in the enzyme incubations. A series of matrix spikes and standard addition experiments were performed in order to evaluate precision and accuracy (or bias due to sample matrix) of the present method. In the matrix spike experiments, both phosphate buffer and rat serum were spiked to yield a final concentration of ~3, 20, and 50 nM of each analyte, extracted and analyzed. The resulting concentrations were compared with standard addition experiments in which the samples were fortified with 0, 3, 20, and 50 nM analyte post extraction. All samples were extracted and analyzed in triplicate. The standard additions (post-extraction fortifications) allowed evaluation of matrix interference on the ability to quantify a known amount of compound. For all the concentrations, analytes were detected accurately with variations ranging from 20 to 50%.

Tissue preparation

Brain and spinal cord tissues (~100 mg) were collected postmortem from male Sprague-Dawley rats (300–350 g). Animals were anesthetized with Nembutal and perfused with cold saline to eliminate blood from the tissues. All samples were flash-frozen with liquid nitrogen and stored at −80°C until used. After thawing and weighing, 10 μL of anti-oxidant solution (0.2 mg/ml of BHT and EDTA), 10 μL of surrogate standards solution, and 400 μl of ice-cold methanol with 0.1% of acetic acid and 0.1% of BHT were added onto the tissue samples and incubated at −80°C for 30 min. Samples were then homogenized by using ultrasonic-homogenizer at 30 Hz for 10 min and centrifuged at 10,000 rpm for 10 min at 4°C. The supernatants were collected and pellets were reextracted with 100 μL of ice-cold methanol with 0.1% of acetic acid and 0.1% of BHT and centrifuged. The supernatant of each extract combined, and an equal volume of 0.2 N $NaHCO_3$ in water was added to hydrolyze lipid esters. The mixtures were allowed to react at 4°C overnight. The solutions were then acidified with 1.5 ml of 0.2 N acetic acid in water and loaded onto solid phase extraction (SPE) cartridges for SPE.

SPE

Oasis cartridges (Waters) were washed with ethyl acetate and methanol and equilibrated with [20% methanol (MeOH), 80% water] to the initial condition. Diluted supernatants of the samples were loaded on the cartridges and washed twice with SPE solution (water with 20% MeOH). The cartridges were dried under vacuum followed by elution using 0.5 ml of methanol and 3 ml of ethyl acetate into tubes with 10 μL of trapping solution (30% glycerol in MeOH). The eluates were dried by vacuum and reconstituted with an internal standard solution. Recovery for the epoxide surrogate (D_{11} 11,12-EET) was 77%, and recovery for the diol surrogate (D_{11} 14,15-DHET) was 82%. No D_{11} 11,12-DHET (the diol resulting from the epoxide surrogate) was detected, indicating that no significant hydrolysis of the epoxides took place during the sample preparation and analysis. This is consistent with previous observations (28).

Kinetic assay conditions

Kinetic parameters for a series of monoepoxy-fatty acids were determined under steady-state conditions using the purified recombinant human sEH (30, 31). One μl of substrate solution in ethanol ($[S]_{final}$ from 1.0 to 50 μM; 7 to 8 concentrations used for each substrate) was added to 100 μl of the enzyme solution at 0.2 μg/ml ($[E]_{final} \approx 3$ nM) in Bis-Tris HCl buffer (25 mM, pH 7.0) containing 0.1 mg/ml of lipid free BSA. The reaction mixtures were incubated at 30°C for 5 to 15 min. The reactions were then quenched by adding 400 μl of methanol and 1 μl of internal standard (9,10-dihyoxy-heptadecanoic acid). The quantity of diol formed was then determined by LC/MS/MS analysis as described above. The kinetic constants (K_M and V_m) were calculated by nonlinear fitting of the Michaelis equation using the enzyme kinetic module of SigmaPlot version 9.01 (Systat Software Inc., Chicago IL). The k_{cat} constant was then calculated from V_m using a concentration of enzyme of 3 nM.

Behavioral nociceptive testing

This study was approved by University of California Davis Animal Care and Use Committee. Male Sprague-Dawley rats weighing 250–300 g were obtained from Charles River Inc., and maintained in UC Davis animal housing facilities with ad libitum water and food on a 12 h:12 h light-dark cycle. Data were collected during the same time of day for all groups. Behavioral nociceptive testing was conducted as described previously by assessing thermal hind paw withdrawal latencies using a commercial Hargreaves apparatus (32) and by assessing mechanical withdrawal threshold using an electronic Von Frey anesthesiometer apparatus (IITC, Woodland Hills, CA). Three measurements were taken at 1 to 2 min interstimulus intervals. Mean area under the normalized time-response curve (0–120 min after intraplantar compound administration) was calculated using the trapezoidal method and areas under the time-response curve in arbitrary units are presented in the figures. Data were normalized to percentage values using the formula: (thermal withdrawal latency at time point × 100)/ thermal withdrawal latency before treatment. For the mechanical withdrawal threshold measurements, the controller was set to 'maximum holding' mode so that the highest applied force (in grams) upon withdrawal of the paw was displayed. EET, EpDPE, and EpETE were tested using the intraplantar carrageenan elicited pain associated with inflammation model (26) by injecting them directly in the paw or in the spinal cord.

Injection in the paw. Following baseline measurements, carrageenan (50 μl, 1% solution of carrageenan, 0.5 mg) was administered into the plantar area of one hind paw (n = 6 per group). Four hours following this, postcarrageenan responses were determined. Immediately after (t = 0), the vehicle (10% EtOH in saline), the free fatty acids or regioisomeric mixtures of EET, EpDPE, and EpETE methyl esters, or corresponding diols were administered into the same paw by intraplantar injection in a volume of 10 μl vehicle solution in quantities indicated in figure legends, as described before (26). Responses following compound administration were monitored over the course of 2 h.

Injection in the spinal cord. Intrathecal catheters were implanted according to Yaksh and Rudy (33). Following baseline measurements, animals were injected with carrageenan in saline in the plantar surface of one hind paw (0.5 mg; n = 6 per group). Four hours after carrageenan, baseline thermal withdrawal latency and mechanical withdrawal thresholds were measured. Following this, 10 μl of artificial cerebrospinal fluid containing vehicle (1% DMSO) or EpDPE regioisomeric mixture was administered through the catheters (t = 0). After 45 min, thermal withdrawal latency and mechanical withdrawal thresholds were measured again.

Statistics

Results are presented as average ± standard deviation unless noted otherwise. Kinetic parameters were determined by nonlinear regression of the Michaelis-Menten equation using SigmaPlot (v9.01, Systat Software Inc., Chicago, IL). F-test and *t*-test ($P < 0.05$) were performed to ensure the quality of the fitting. Data from nociceptive testing were analyzed using ANOVA followed by Dunnett's 2-sided *t*-test for group comparisons. Statistical significance was set to $P \leq 0.05$.

RESULTS

Occurrence and distribution of epoxy-fatty acids in rat tissues

Several studies established that DHA and EPA can be oxygenated by CYP enzymes in a manner parallel to oxygenation of arachidonic acid (5, 14–17). This prompted us to hypothesize that EpDPEs and EpETEs occur in mammalian tissues. Because n-3 fatty acids are known to accumulate in the central nervous system, we concentrated on the brain and spinal cord. Eicosanoids are known to be incorporated in various lipid esters, affecting their bioactivity (34). Because fatty acids and their metabolites could still be released from membranes postmortem (35), we measured total oxylipin concentrations after base hydrolysis of the lipid esters. As presented in **Table 1**, these organs contained significantly more EpDPE than EpETE, consistent with the observation that there is more DHA than EPA in the central nervous system (CNS) (36). Although only the 17,18-EpETE regioisomer of parent EPA was detected in the brain and spinal cord, all of the EpDPE regioisomers of parent DHA were present. Except for the 7,8-EpDPE, which was present in relatively high quantity compared with the other epoxy-fatty acids, the EpETEs in the CNS were in similar quantities to the EET regioisomers (Table 1). Similarly, for the C_{18} fatty acids, the n-3 α-EpODEs were present in similar quantities to the n-6 EpOME.

Kinetic constants of epoxy-fatty acids for the human sEH

Next, based on the ability of sEH to hydrolyze epoxy C:18 (EpO and EPOME) and C:20 fatty acids (EET), we hypothesized that EpODE, EpDPE, and EpETE might also be hydrolyzed by sEH (28). We tested this hypothesis by using individual regioisomers of these fatty acids and recombinant human sEH, quantitatively measuring the products, corresponding diols, with the LC-MS/MS method described above. As shown in **Table 2**, all epoxy-fatty acids tested were substrates for the human sEH though significant differences were observed. The results for all the substrates tested fitted well with the Michaelis-Menten equation ($r^2 > 0.94$; **Fig. 1**). Although apparently better fitting (higher r^2) was obtained with a cooperative model (37), the velocity values calculated from the cooperative model were not statistically different ($P > 0.05$) than the values obtained with the Michaelis model. This suggests that the apparent better fitting with the cooperative model is an artifact. Because the sEH has a two-step mechanism involving the formation and hydrolysis of a covalent intermediate (38), K_M in this case was not a measure of the affinity of the substrate for the enzyme. Rather, K_M reflects the concentration of substrate for which the velocity is half maximal. As expected, using various epoxy-fatty acids, we observed increases of the observed K_M values with a parallel increase in k_{cat} values. However, 8,9-EET, 8,9-EpETE, and 19,20-EpDPE are exceptions to this rule

TABLE 1. Rat tissue content of fatty acid monoepoxides

	Brain		Spinal Cord	
	Epoxide	Diol	Epoxide	Diol
Abbreviation	Tissue Concentration (pmol/mg tissue)			
9,10-EpOME	2.8 ± 0.1	1.3 ± 0.2	3.7 ± 0.7	5.4 ± 0.3
12,13-EpOME	2.7 ± 0.2	2.9 ± 0.6	3.1 ± 0.8	6.6 ± 1.2
α 9,10-EpODE	1.3 ± 0.2	0.2 ± 0.1	3.1 ± 0.8	0.3 ± 0.1
α 12,13-EpODE	2.9 ± 0.6	BLD	6.6 ± 1.2	BLD
α 15,16-EpODE	0.2 ± 0.1	1.6 ± 0.2	0.2 ± 0.1	5.0 ± 1.40
5,6-EET	7 ± 1	BLD	13 ± 13	BLD
8,9-EET	4 ± 2	0.35 ± 0.04	7 ± 6	0.5 ± 0.1
11,12-EET	11 ± 1	0.6 ± 0.1	17 ± 13	0.5 ± 0.1
14,15-EET	6.3 ± 0.6	1.2 ± 0.2	10 ± 8	1.0 ± 0.2
8,9-EpETE	BLD	BLD	BLD	BLD
11,12-EpETE	BLD	BLD	BLD	BLD
14,15-EpETE	BLD	0.11 ± 0.02	BLD	0.3 ± 0.2
17,18-EpETE	0.3 ± 0.2	1.4 ± 0.4	1.2 ± 0.8	1.4 ± 0.3
7,8-EpDPE	104 ± 28	BLD	76 ± 12	BLD
10,11-EpDPE	3.5 ± 0.5	0.4 ± 0.1	3 ± 3	0.43 ± 0.02
13,14-EpDPE	2.0 ± 0.5	0.3 ± 0.1	2 ± 1	0.5 ± 0.1
16,17-EpDPE	1.7 ± 0.1	0.7 ± 0.6	2 ± 1	1.3 ± 0.2
19,20-EpDPE	4.0 ± 0.7	5.3 ± 0.8	5 ± 3	8 ± 6

Animals were sacrificed and perfused with cold saline. Tissues were excised and extracted two times with acidified methanol, followed by base hydrolysis of the lipid esters. Surrogates were added before extraction. Extracts were further purified using C18 SPE cartridges. Internal standards were added and samples were subjected to LC/MS/MS analysis. Surrogates recoveries of ~80% were obtained. Values are tissue average ± standard deviation (n = 3). The abbreviations used for oxidized fatty acids follow the recommendations of Smith (47), adopted by the International Union of Pure and Applied Chemistry (IUPAC). BLD, below the limit of detection of 0.1 pmol/mg of tissue.

TABLE 2. Kinetic constants of recombinant purified human sEH for epoxy-fatty acids

Substrate	Parent Fatty Acid	K_M(μM)	k_{cat}(s^{-1})	$r^{2\,a}$	k_{cat}/K_M($s^{-1}\mu M^{-1}$)	Preference Index[b]
cis 9,10-EpO	C18:1	1.1 ± 0.1	0.079 ± 0.001	0.98	0.075 ± 0.009	1.0
trans 9,10-EpO		0.7 ± 0.2	0.053 ± 0.002	0.98	0.09 ± 0.03	1.2
9,10-EpOME	C18:2	2.6 ± 0.4	0.72 ± 0.06	0.98	0.28 ± 0.02	3.7
12,13-EpOME		3.1 ± 0.2	0.73 ± 0.03	0.94	0.24 ± 0.01	3.2
α 9,10-EpODE	αC18:3	5.0 ± 0.3	0.51 ± 0.01	0.99	0.101 ± 0.004	1.3
α 12,13-EpODE		15.5 ± 0.9	1.32 ± 0.04	0.98	0.085 ± 0.002	1.1
α 15,16-EpODE		10.3 ± 0.7	1.21 ± 0.02	0.95	0.118 ± 0.006	1.6
γ 6,7-EpODE	γC18:3	3.9 ± 0.1	0.118 ± 0.003	0.97	0.030 ± 0.001	0.4
γ 9,10-EpODE		3.9 ± 0.1	0.65 ± 0.01	0.98	0.128 ± 0.006	1.7
γ 12,13-EpODE		1.8 ± 0.1	0.36 ± 0.03	0.99	0.199 ± 0.006	2.6
8,9-EET	C20:4	26 ± 1	0.56 ± 0.03	0.97	0.022 ± 0.001	0.3
11,12-EET		2.0 ± 0.1	0.26 ± 0.01	0.97	0.13 ± 0.01	1.7
14,15-EET		7.0 ± 0.3	3.0 ± 0.1	0.95	0.43 ± 0.01	5.7
8,9-EpETE	C20:5	24.6 ± 0.4	0.74 ± 0.02	0.94	0.030 ± 0.001	0.4
11,12-EpETE		3.6 ± 0.5	0.83 ± 0.01	0.97	0.23 ± 0.03	3.1
14,15-EpETE		9.3 ± 0.5	2.40 ± 0.04	0.95	0.26 ± 0.01	3.5
17,18-EpETE		9.7 ± 0.4	1.18 ± 0.02	0.95	0.12 ± 0.01	1.6
7,8-EpDPE	C22:6	15 ± 2	0.58 ± 0.04	0.98	0.038 ± 0.001	0.5
10,11-EpDPE		5.1 ± 0.5	2.45 ± 0.03	0.94	0.49 ± 0.05	6.5
13,14-EpDPE		3.1 ± 0.3	2.85 ± 0.09	0.96	0.92 ± 0.07	12.7
16,17-EpDPE		3.3 ± 0.2	1.91 ± 0.02	0.94	0.58 ± 0.03	7.7
19,20-EpDPE		36 ± 2	0.62 ± 0.03	0.95	0.017 ± 0.001	0.2

Recombinant human sEH was expressed in insect cells using a baculovirus vector. The enzyme was purified using affinity chromatography. Each substrate was tested in 7-8 concentrations. Reaction product diols were then quantified by LC-MS/MS. Results are average ± standard deviation (n = 3).

[a] overall value;

[b] k_{cat}/K_M ratios.

because they have relatively poor K_M (>25 μM) with intermediate k_{cat}s. The second step of the sEH reaction mechanism is at least an order of magnitude slower than the first step (38). Thus, k_{cat} values represent largely the rate of hydrolysis of the covalent intermediate. However, the k_{cat} of the EpOs, those that are from monounsaturated fatty acids (MUFAs), were much smaller than those from the PUFAs, suggesting that intermediate formation could be rate limiting for the MUFA. For the PUFA, k_{cat} values varied an order of magnitude depending on the position of the epoxide on the fatty acid structure. In general, k_{cat}s were the largest when the epoxide was on the 14th or 15th carbon of the fatty acid chain.

The ratio k_{cat}/K_M is a specific measurement of the overall rate of the reaction for a particular substrate. Using this ratio and its value for *cis* 9,10-EpO as a reference, a relative preference index was calculated. More than a 60-fold difference between the best (13,14-EpDPE) and the worst substrate (19,20-EpDPE) was evident. Overall, it was clear that the sEH preferred epoxides situated in the middle of the fatty acid chain, and that its activity decreased significantly if the epoxide was closer to the acid function or the ω-carbon. This preference probably reflects the structure of the human sEH active site, which is proposed to have large hydrophobic pockets on either side of the catalytic residues (38). For the EpOME and EET, the rodent and human sEH showed similar preferences (28). Thus, one could assume that these two enzymes will have overall similar preferences for all the epoxy-fatty acids studied herein. When comparing n-6 to n-3 epoxy-fatty acids in either the α- and γ-epODE or the EET to the EpETE series, there was no clear preference for any particular kind of fatty acid. Although overall sEH seemed to prefer EpDPE over EET, it is clear that in vivo inhibition of sEH will affect the metabolism of all of these epoxy-fatty acids, and the extent of this effect will mostly depend on the relative abundance of each regioisomer.

EETs, EpDPEs, and EpETEs are peripherally acting antihyperalgesic molecules

Next, we tested the hypothesis that EpDPEs are analogous to EETs in function. One of the landmark bioactivities of EETs and sEH inhibitor is their strong antihyperalgesic effects (26, 32). Because EpDPE and EpETE are apparently better substrates for sEH than EET, we hypothesized that they may also have better antihyperalgesic effects.

We tested this hypothesis using the carrageenan elicited local pain associated with inflammation model (26). Carrageenan administration, as expected, significantly (>4-fold) decreased both thermal withdrawal latencies and mechanical withdrawal thresholds (**Fig. 2**). We previously showed that the carrageenan painful effect lasts at least 8 h (26). The bioactivity of regioisomeric mixtures of EETs, EpETEs, and EpDPEs were then determined. Intraplantar administration of a low dose of 300 ng/paw of the epoxy-fatty acids resulted in significant antihyperalgesic activity that lasted for at least 2 h. Among the epoxy-fatty acids, the EpDPEs were surprisingly the most effective in reducing pain associated with inflammation, followed by the EETs and the EpETEs (Fig. 2A, B). By contrast, the parent free fatty acids were inactive even when administered at 10-fold higher quantity (3,000 ng/paw; Fig. 2C), and the corresponding diols were also inactive when administered at an identical dose (300 ng/paw; data not shown). Overall, these data support the hypothesis that epoxygenated metabolites are involved in pain signaling.

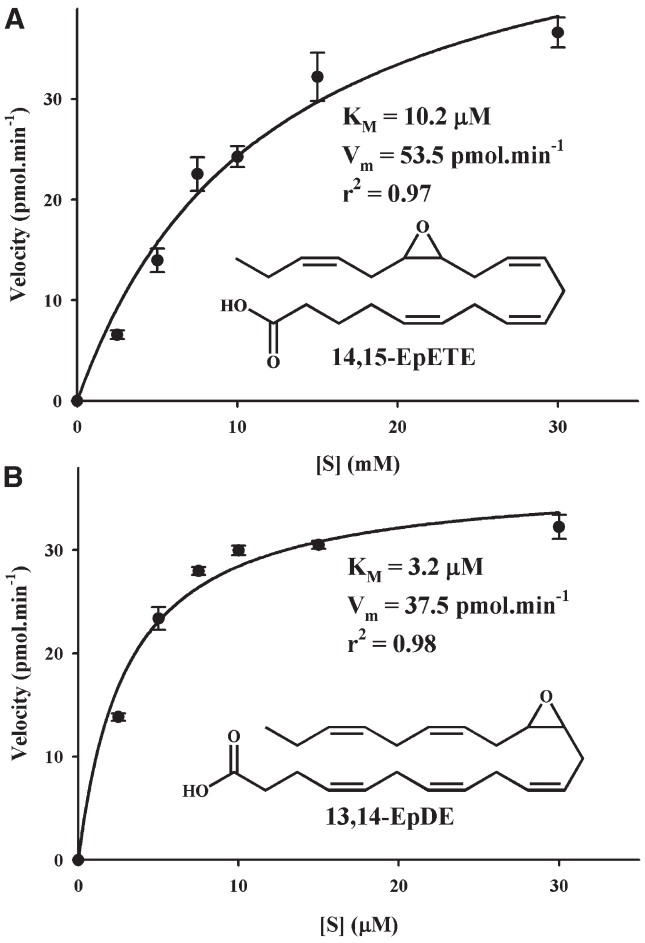

Fig. 1. Determination of the kinetic constants for 14,15-EpETE (A) and 13,14-EpDPE (B) with the human sEH($[E]_{final} \approx 3$ nM) in Bis-Tris HCl buffer (25 mM, pH 7.0) containing 0.1 mg/ml of lipid free BSA at 30°C. The kinetic constants (K_M and V_m) were calculated by nonlinear fitting of the Michaelis equation using the enzyme kinetic module of SigmaPlot version 9.01 (Systat Software Inc., Chicago, IL).

We then investigated whether individual regioisomers of EpDPE were active because there were different quantities of each regioisomer in the spinal cord and the brain. Three regioisomers were selected based on information presented in Table 2. Even though each regioisomer was active, there were significant differences among the regioisomers (Fig. 2D). The position of the epoxide functionality was important in the antihyperalgesic activity. The rank order of efficacy in reducing pain associated with inflammation (13,14-EpDPE > 16,17-EpDPE > 19,20-EpDPE) was in parallel to the rank order of preference by the sEH (Table 2).

EPDPEs are also antihyperalgesic in the central nervous system

Because the EpDPEs had significant peripheral antihyperalgesic activity, we investigated whether the EpDPEs were also active in the CNS. We administered the regioisomeric mixture of EpDPE into the spinal cord through chronically implanted intrathecal catheters, first to noninflamed animals and then to carrageenan inflamed animals. The EpDPE (3 μg/animal) did not change thermal withdrawal latency or mechanical withdrawal threshold of noninflamed animals ($P > 0.1$ for both tests, not shown). However, they were highly efficacious when administered into the spinal cord of inflamed animals (**Fig. 3**). This high concentration of EpDPE completely reversed the decrease in thermal withdrawal latency and partially reversed mechanical withdrawal threshold. These findings indicate a selective role of the epoxides of DHA in modulating nociceptive physiology.

DISCUSSION

Many of the past efforts on bioactive lipids focused on ARA metabolites and their biological relevance (8, 13, 25). Here, we report on the presence, distribution, and regulation of the levels by sEH of a set of 18, 20, and 22 carbon epoxy-fatty acids in both n-3 and n-6 series. We also report a direct antinociceptive role for n-3 epoxy-fatty acid metabolites and more specifically those of DHA.

Lipid molecules are ubiquitous messengers that are known to participate in intracellular signaling, cell-to-cell communication, serve as neurotransmitters, and regulate specific physiologic functions, one of which is the transmission of noxious sensory information both in the periphery and the CNS (1, 9, 25, 39). Analysis of alterations in the type, amount, and organization of lipids can thus provide critical information leading to the understanding of mechanism of action of each molecule, diagnostic tools, therapeutic strategies, and identification of the mechanisms underlying the disease processes. Analytical methods based on LC/MS technology are highly sensitive methods that simultaneously provide information on quantity and identity of multiple analytes in a complex sample (28). Accordingly, the methods developed herein show promise in the quantitative analysis of epoxy-fatty acids both from in vitro experiments and from tissue extracts. Using this technology, we studied the role of n-3 epoxy-fatty acids in nociceptive pathophysiology.

sEH efficiently degrades n-3 and n-6 series epoxy-fatty acids

In mammals, the sEH was historically found in liver, kidneys, and at lower levels in other organs (25). Recently, the sEH was found in the brain, specifically in astrocytes and in the body of the neuronal cells (40, 41). The sEH is the primary mammalian enzyme that degrades EET in vivo (25). In murine brain, sEH is responsible for at least two-thirds of the EET hydrolysis (41). Pharmacological inhibition of sEH has been demonstrated to stabilize EETs and is being considered as a potential therapeutic approach for hypertension, vascular inflammation, and pain (10, 13, 26, 27). Inhibition of sEH is beneficial also in ischemic brain injury and stroke (42).

Although it was not surprising that sEH would degrade epoxy-fatty acids other than those in the C_{18} and C_{20} n-6 series such as the EET and EpOME, an unexpected outcome of this study was that EpDPE and EpETE are in fact degraded efficiently by sEH (Table 2) (25). We showed

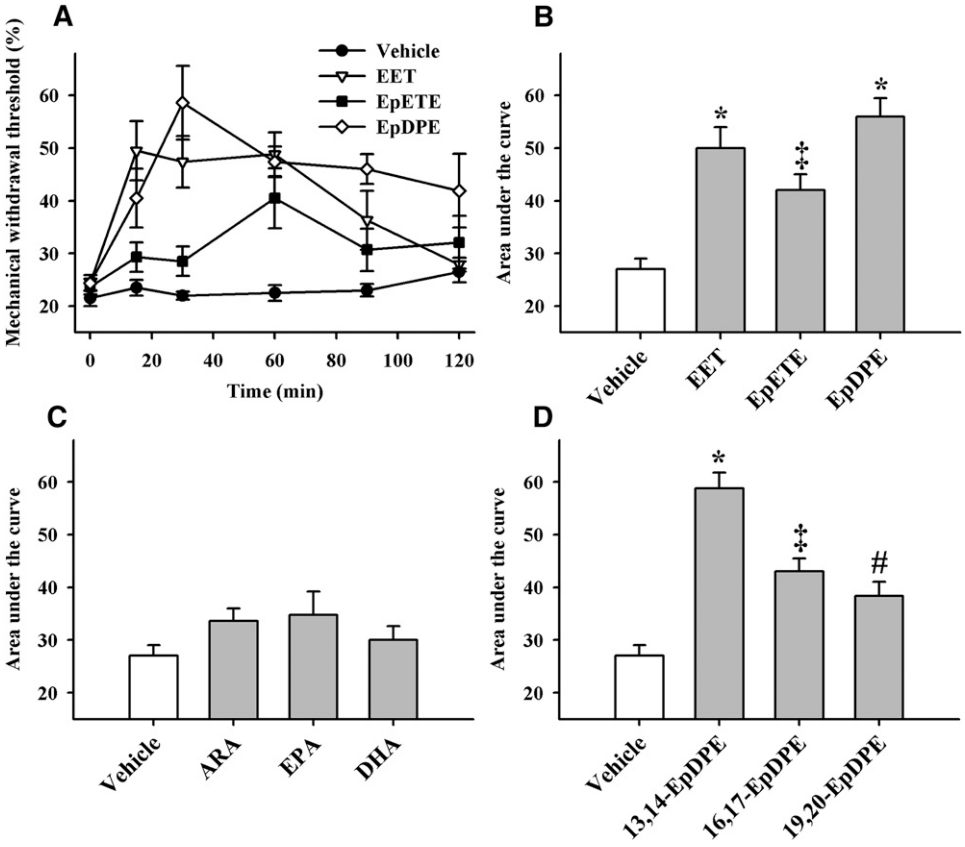

Fig. 2. Epoxy-fatty acids but not parent fatty acids reduce pain associated with inflammation induced by a single intraplantar injection of 0.5 mg of carrageenan in rat paws (n = 6 per group). A: Regioisomeric mixtures of EET, EpETE, and EpDPE (300 ng /paw) all significantly reversed carrageenan induced pain ($P < 0.01$), measured as a percent of mechanical withdrawal thresholds before inflammation. The EET and the EpETE gave a significant action for 90 min, while EpDPE were still significantly active after 120 min. B: The area under the curve (integrated from 0–120 minutes), which gives an overall measurement of the efficacy of a treatment, is reported on the *y* axis for each compound from panel A. Compared with the vehicle control (10% ethanol in saline), the mixture of epoxy-fatty acids significantly reduced the pain (* $P < 0.001$; ‡ $P < 0.01$). EpETE had lower efficacy than EpDPE ($P = 0.009$) but not lower than EET ($P = 0.12$). C: The parent free fatty acids (ARA, EPA, and DHA) at 3000 ng/paw, failed to significantly reduce pain ($P = 0.1$). D: All three individual EpDPE regioisomers (300 ng /paw) tested significantly reduced pain (* $P < 0.001$; ‡ $P = 0.001$; # $P = 0.03$, compared with the vehicle). 16, 17-EpDPE and 19,20-EpDPE were similar in efficacy ($P = 0.29$), whereas 13,14-EpDPE was more efficacious than them ($P < 0.01$).

that the epoxides of EPA and DHA are indeed preferred substrates for sEH over the other epoxy-fatty acids tested including the EET and EpOME. Thus, in vivo inhibition of sEH or an alteration in its titer will not only affect the metabolism of EETs and EpOME but also the metabolism and bioactivity of EpDPE and EpETE. Obviously, the extent of such an effect will depend on the relative abundance of each epoxy-fatty acid in addition to the extent of their respective interactions with molecular targets. Although EPA concentrations are relatively low in the body, DHA concentrations, especially in neuronal and retinal tissues, are similar to or higher than those of ARA (36). Accordingly, in rat brain and spinal cord we did not find detectable levels of EpETE, but we found similar and significant amounts of EET and EpDPE (Table 1). Although representing a small amount of the parent fatty acid, the EET are very bioactive (8, 10). Our data suggest a similar scenario for the DHA epoxides. Taken together, these data suggest that pharmacological inhibition of sEH will affect EpDPE levels in the brain similarly to the way it affects EET levels (41, 42). Like the EET (34), it is likely that under normal physiologic conditions sizable amounts of EpDPE are esterified in lipids. These esters could have direct biological activities or act as stores from which the oxylipins could be released.

n-3 Series epoxy-fatty acid regioisomers are selectively antihyperalgesic

A significant aspect of the role of lipids in neuronal function is their ability to modify the functional responses of ion channels, synaptic transmission, and cellular signaling cascades through which neuronal cell function is altered to meet physiologic demand (39). We previously showed that the EET are antihyperalgesic in inflammatory and neuropathic pain models (26, 32, 43). Furthermore, the pharmacological inhibition of sEH, which resulted in the stabilization of the EET levels, is also strongly antihyperalgesic (32, 43). In this study, we demonstrate that n-3

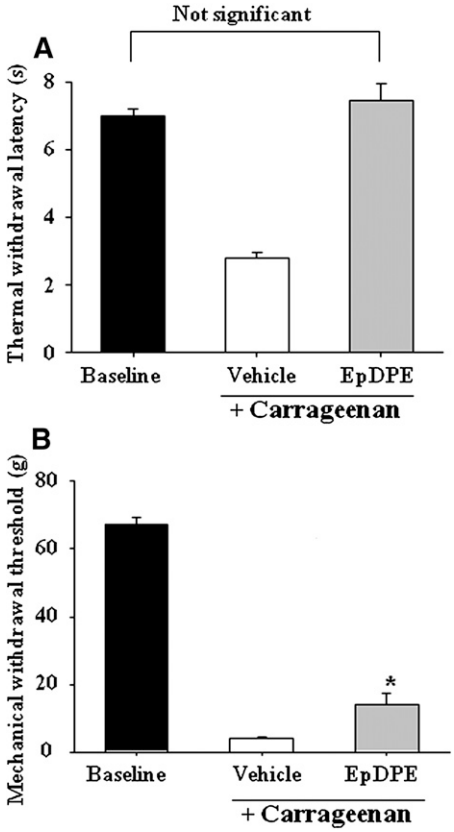

Fig. 3. Spinal administration of EpDPE reduces both mechanical and thermal pains associated with inflammation induced by a single intraplantar injection of 0.5 mg of carrageenan in rat paws (n = 6 per group). Measurements were made 45 min after injection into the spinal cord. A: Compared with vehicle (1% DMSO in artificial cerebrospinal fluid), EpDPEs (3,000 ng/animal) significantly reversed the decreased thermal withdrawal latency ($P < 0.001$) to baseline levels ($P = 0.59$). B: Compared with vehicle, EpDPEs reversed the decrease in mechanical withdrawal threshold ($P < 0.001$), though it did not reach baseline level ($P < 0.001$).

epoxy-fatty acids are also strongly antihyperalgesic, especially EpDPE (Fig. 2). Because no sEH inhibitors were used, the epoxy-fatty acids injected in the paw probably hydrolyzed by sEH to the diols, which are not active. This could explain the slow reduction of the efficacy of the compounds over the length of the experiment (2 h). Although EpDPE and EET displayed a similar efficacy in reducing pain (~50%; Fig. 2A, B), the DHA epoxides acted longer. The EpETEs were less effective than the EETs. The EETs and EpDPEs have strong peripheral anti-hyperalgesic properties with potencies similar to the endocannabinoids (43, 44). For example, a 300 ng dose EpDPE regioisomer mixture gave a similar reduction in pain as 75 ng of anandamide in a similar model (44). Given the intensity of the painful state induced by carrageenan, the observed effects are highly significant.

Because the bioactivity of the regioisomers of EET vary dramatically in assays for angiogenesis, inflammation, and vasodilatation (45) and the EpDPE regioisomers aare not uniformly distributed in rat tissues (Table 1), we evaluated the ability of EpDPE regioisomers in reducing pain. There were significant differences in the ability of the regioisomers to decrease pain associated with inflammation (Fig. 2D). Because the 11,12- and 14,15-EET are the most effective mediators of the above biology (45), it was not surprising that the antihyperalgesic activity is related to the position of the epoxide functionality among the EpDPE regioisomers. The rank order of potency of the tested EpDPE regioisomers is 13,14-EpDPE > 16,17-EpDPE > 19,20-EpDPE, with a clear decline in biological activity as the epoxide function is moved further from the acid function (Fig. 2D). At the same time, this rank order of antihyperalgesic effects remarkably follows the preference of the sEH for these substrate molecules (Table 2). This trend was previously observed for the biological activity of the EET regioisomers (25, 45).

The sEH is expressed in the CNS, particularly in neurons and astrocytes of the brain (41). Even though spinal expression of sEH has not been demonstrated by immunohistochemistry (40), we detected a considerable quantity of sEH mRNA in whole spinal cord. Consistent with the presence of sEH in the spinal cord, we report the presence of epoxy-fatty acids and their corresponding diols in the spinal cord (Table 1). Our earlier work suggested that the antihyperalgesic effect of sEH inhibitors are at least partially mediated by the CNS. Here, those earlier observations are supported because EpDPE effectively eliminated thermal hyperalgesia when administered into the spinal cord (Fig. 3). The differential effects of peripheral and spinal administration of EpDPE in thermal versus mechanical withdrawal tests imply a selective mechanism of action of the EpDPE because these responses were shown to be mediated by different types of neurons (44, 46).

Although the detail mechanism(s) by which epoxy-fatty acids lead to antihyperalgesia is still under investigation (43), it is hypothetically possible that, because of their structural similarity, EET, EpETE, and EpDPE will affect a limited number of molecular targets. Our findings support this concept given that the antihyperalgesic activity reported herein is regioisomer selective (Fig. 2D). Furthermore, the parent fatty acids as well as the corresponding diols had no effect even when administered at higher doses, supporting the selectivity of the biological activity observed. We previously showed that the EET lead to antihyperalgesia in both inflammatory and neuropathic pain states by at least two spinal mechanisms; first, by repressing the induction of the COX2 gene and second, by rapidly upregulating an acute neurosteroid-producing gene, StARD1 (43). We hypothesize that EpETE and EpDHE are antihyperalgesic through mechanisms similar to that of the EET.

At least theoretically, inhibition or downregulation of sEH in vivo is expected to result in increased levels of multiple different epoxy-fatty acids (25). For the linoleic and arachidonic epoxy-fatty acids this is the most frequently observed outcome. Although in other cases when sEH is inhibited, a decrease in sEH products, the corresponding diols of EET and EpOME, is observed (25). Data presented here clearly suggest EpDPE and EpETE should be taken into consideration when sEH inhibitors are used in various disease models. If inhibition of sEH results in the

stabilization of a wide range of epoxy-fatty acids, then investigating the individual epoxy-fatty acids and their regio- and stereoisomers should increasingly provide insight into the pleitropic effects of inhibiting sEH such as antihypertensive and anti-inflammatory effects (27). Here, we demonstrated the presence and bioactivity of epoxy-fatty acid regioisomers and the preference of sEH toward these substrates, indicating that both sEH and fatty acid epoxides are involved in the same system of chemical mediation. In summary, the parent fatty acids DHA and EPA are receiving increasing attention in particular in regard to their beneficial effects on cardiovascular and neurological systems. However, given that CYPs efficiently convert DHA and EPA to their epoxygenated metabolites (5, 17), the EpDPEs and EpETEs are likely to be responsible for at least some of the beneficial effects associated with dietary DHA and EPA.

REFERENCES

1. Harris, W. S., P. M. Kris-Etherton, and K. A. Harris. 2008. Intakes of long-chain omega-3 fatty acid associated with reduced risk for death from coronary heart disease in healthy adults. *Curr. Atheroscler. Rep.* **10:** 503–509.
2. Fedor, D., and D. S. Kelley. 2009. Prevention of insulin resistance by n-3 polyunsaturated fatty acids. *Curr. Opin. Clin. Nutr. Metab. Care.* **12:** 138–146.
3. Goldberg, R. J., and J. Katz. 2007. A meta-analysis of the analgesic effects of omega-3 polyunsaturated fatty acid supplementation for inflammatory joint pain. *Pain.* **129:** 210–223.
4. Tjonahen, E., S. F. Oh, J. Siegelman, S. Elangovan, K. B. Percarpio, S. Hong, M. Arita, and C. N. Serhan. 2006. Resolvin E2: identification and anti-inflammatory actions: pivotal role of human 5-lipoxygenase in resolvin E series biosynthesis. *Chem. Biol.* **13:** 1193–1202.
5. Fer, M., Y. Dréano, D. Lucas, L. Corcos, J. P. Salaün, F. Berthou, and Y. Amet. 2008. Metabolism of eicosapentaenoic and docosahexaenoic acids by recombinant human cytochromes P450.). *Arch. Biochem. Biophys.* **471:** 116–125.
6. Harmon, S. D., X. Fang, T. L. Kaduce, S. Hu, V. Raj Gopal, J. R. Falck, and A. A. Spector. 2006. Oxygenation of omega-3 fatty acids by human cytochrome P450 4F3B: effect on 20-hydroxyeicosatetraenoic acid production. *Prostaglandins Leukot. Essent. Fatty Acids.* **75:** 169–177.
7. Jump, D. B. 2002. The biochemistry of n-3 polyunsaturated fatty acids. *J. Biol. Chem.* **277:** 8755–8758.
8. Capdevila, J. H., J. R. Falck, and R. C. Harris. 2000. Cytochrome P450 and arachidonic acid bioactivation. Molecular and functional properties of the arachidonate monooxygenase. *J. Lipid Res.* **41:** 163–181.
9. Das, U. N. 2006. Essential fatty acids: biochemistry, physiology and pathology. *Biotechnol. J.* **1:** 420–439.
10. Gauthier, K. M., W. Yang, G. J. Gross, and W. B. Campbell. 2007. Roles of epoxyeicosatrienoic acids in vascular regulation and cardiac preconditioning. *J. Cardiovasc. Pharmacol.* **50:** 601–608.
11. Serhan, C. N., and J. Savill. 2005. Resolution of inflammation: the beginning programs the end. *Nat. Immunol.* **6:** 1191–1197.
12. Serhan, C. N., and N. Chiang. 2007. Endogenous pro-resolving and anti-inflammatory lipid mediators: a new pharmacologic genus. *Br. J. Pharmacol.* **153:** S200–S215.
13. Spector, A. A., and A. W. Norris. 2006. Action of epoxyeicosatrienoic acids on cellular function. *Am. J. Physiol. Cell Physiol.* **292:** C996–C1012.
14. VanRollins, M., R. C. Baker, H. W. Sprecher, and R. C. Murphy. 1984. Oxidation of docosahexaenoic acid by rat liver microsomes. *J. Biol. Chem.* **259:** 5776–5783.
15. VanRollins, M., P. D. Frade, and O. A. Carretero. 1989. Synthesis of epoxide and vicinal diol regioisomers from docosahexaenoate methyl esters. *J. Lipid Res.* **30:** 275–286.
16. Yamane, M., A. Abe, and S. Yamane. 1994. High-performance liquid chromatography-thermospray mass spectrometry of epoxy polyunsaturated fatty acids and epoxyhydroxy polyunsaturated fatty acids from an incubation mixture of rat tissue homogenate. *J. Chromatogr. A.* **652:** 123–136.
17. Barbosa-Sicard, E., M. Markovic, H. Honeck, B. Christ, D. N. Muller, and W. H. Schunck. 2005. Eicosapentaenoic acid metabolism by cytochrome P450 enzymes of the CYP2C subfamily. *Biochem. Biophys. Res. Commun.* **329:** 1275–1281.
18. Lauterbach, B., E. Barbosa-Sicard, M-H. Wang, H. Honeck, E. Kargel, J. Theuer, M. L. Schwartzman, H. Haller, F. C. Luft, M. Gollasch, et al. 2002. Cytochrome P450-dependent eicosapentaenoic acid metabolites are novel BK channel activators. *Hypertension.* **39:** 609–613.
19. Ye, D., D. Zhang, C. Oltman, K. Dellsperger, H-C. Lee, and M. VanRollins. 2002. Cytochrome p-450 epoxygenase metabolites of docosahexaenoate potently dilate coronary arterioles by activating large-conductance calcium-activated potassium channels. *J. Pharmacol. Exp. Ther.* **303:** 768–776.
20. Morin, C., M. Sirois, V. Echave, E. Rizcallah, and E. Rousseau. 2009. Relaxing effects of 17(18)-EpETE on arterial and airway smooth muscles in human lung. *Am. J. Physiol. Lung Cell. Mol. Physiol.* **296:** L130–L139.
21. McLennan, P., P. Howe, M. Abeywardena, R. Muggli, D. Raederstorff, M. Mano, T. Rayner, and R. Head. 1996. The cardiovascular protective role of docosahexaenoic acid. *Eur. J. Pharmacol.* **300:** 83–89.
22. Hashimoto, M., K. Shinozuka, S. Gamoh, Y. Tanabe, M. S. Hossain, Y. M. Kwon, N. Hata, Y. Misawa, M. Kunitomo, and S. Masumura. 1999. The hypotensive effect of docosahexaenoic acid is associated with the enhanced release of ATP from the caudal artery of aged rats. *J. Nutr.* **129:** 70–76.
23. Frenoux, J-M. R., E. D. Prost, J. L. Belleville, and J. L. Prost. 2001. A polyunsaturated fatty acid diet lowers blood pressure and improves antioxidant status in spontaneously hypertensive rats. *J. Nutr.* **131:** 39–45.
24. VanRollins, M. 1995. Epoxygenase metabolites of docosahexaenoic and eicosapentaenoic acids inhibit platelet aggregation at concentrations below those affecting thromboxane synthesis. *J. Pharmacol. Exp. Ther.* **274:** 798–804.
25. Newman, J. W., C. Morisseau, and B. D. Hammock. 2005. Epoxide hydrolases: their roles and interactions with lipid metabolism. *Prog. Lipid Res.* **44:** 1–51.
26. Inceoglu, B., K. R. Schmelzer, C. Morisseau, S. L. Jinks, and B. D. Hammock. 2007. Soluble epoxide hydrolase inhibition reveals novel biological functions of epoxyeicosatrienoic acids (EETs). *Prostaglandins Other Lipid Mediat.* **82:** 42–49.
27. Morisseau, C., and B. D. Hammock. 2008. Gerry Brooks and epoxide hydrolases: four decades to a pharmaceutical. *Pest Manag. Sci.* **64:** 594–609.
28. Newman, J. W., T. Watanabe, and B. D. Hammock. 2002. The simultaneous quantification of cytochrome P450 dependent linoleate and arachidonate metabolites in urine by HPLC-MS/MS. *J. Lipid Res.* **43:** 1563–1578.
29. Morisseau, C., M. H. Goodrow, J. W. Newman, C. E. Wheelock, D. L. Dowdy, and B. D. Hammock. 2002. Structural refinement of inhibitors of urea-based soluble epoxide hydrolases. *Biochem. Pharmacol.* **63:** 1599–1608.
30. Wixtrom, R. N., M. H. Silva, and B. D. Hammock. 1988. Affinity purification of cytosolic epoxide hydrolase using derivatized epoxy-activated Sepharose gels. *Anal. Biochem.* **169:** 71–80.
31. Beetham, J. K., T. Tian, and B. D. Hammock. 1993. cDNA cloning and expression of a soluble epoxide hydrolase from human liver. *Arch. Biochem. Biophys.* **305:** 197–201.
32. Inceoglu, B., S. L. Jinks, K. R. Schmelzer, T. Waite, I-H. Kim, and B. D. Hammock. 2006. Inhibition of soluble epoxide hydrolase reduces LPS-induced thermal hyperalgesia and mechanical allodynia in a rat model of inflammatory pain. *Life Sci.* **79:** 2311–2319.
33. Yaksh, T. L., and T. A. Rudy. 1976. Chronic catheterization of the spinal subarachnoid space. *Physiol. Behav.* **17:** 1031–1036.
34. Shearer, G. C., and J. W. Newman. 2009. Impact of circulating esterified eicosanoids and other oxylipins on endothelial function. *Curr. Atheroscler. Rep.* **11:** 403–410.
35. Golovko, M. Y., and E. J. Murphy. 2008. An improved LC-MS/MS procedure for brain prostanoid analysis using brain fixation with head-focused microwave irradiation and liquid-liquid extraction. *J. Lipid Res.* **49:** 893–902.
36. Engström, K., A. S. Saldeen, B. Yang, J. L. Mehta, and T. Saldeen. 2009. Effect of fish oils containing different amounts of EPA,

DHA, and antioxidants on plasma and brain fatty acids and brain nitric oxide synthase activity in rats. *Ups. J. Med. Sci.* **114:** 206–213.
37. Segel, I. H. 1975. Enzyme kinetics, behavior and analysis of rapid equilibrium and steady-state enzyme systems, Willey, New York, NY.
38. Morisseau, C., and B. D. Hammock. 2005. Epoxide hydrolases: mechanisms, inhibitor designs, and biological roles. *Annu. Rev. Pharmacol. Toxicol.* **45:** 311–333.
39. Bazan, N. 2005. Lipid signaling in neural plasticity, brain repair, and neuroprotection. *Mol. Neurobiol.* **32:** 89–103.
40. Sura, P., R. Sura, A. E. Enayetallah, and D. F. Grant. 2008. Distribution and expression of soluble epoxide hydrolase in human brain. *J. Histochem. Cytochem.* **56:** 551–559.
41. Marowsky, A., J. Burgener, J. R. Falck, J-M. Fritschy, and M. Arand. 2009. Distribution of soluble and microsomal epoxide hydrolase in the mouse brain and its contribution to cerebral epoxyeicosatrienoic acid metabolism. *Neuroscience.* **163:** 646–661.
42. Iliff, J. J., and N. J. Alkayed. 2009. Soluble epoxide hydrolase inhibition: targeting multiple mechanisms of ischemic brain injury with a single agent. *Future Neurol.* **4:** 179–199.
43. Inceoglu, B., S. L. Jinks, A. Ulu, C. M. Hegedus, K. Georgi, K. R. Schmelzer, K. Wagner, P. D. Jones, C. Morisseau, and B. D. Hammock. 2008. Soluble epoxide hydrolase and epoxyeicosatrienoic acids modulate two distinct analgesic pathways. *Proc. Natl. Acad. Sci. USA.* **105:** 18901–18906.
44. Reis, G. M., D. Pacheco, A. C. Perez, A. Klein, M. A. Ramos, and I. D. Duarte. 2009. Opioid receptor and NO/cGMP pathway as a mechanism of peripheral antinociceptive action of the cannabinoid receptor agonist anandamide. *Life Sci.* **85:** 351–356.
45. Imig, J. D., and B. D. Hammock. 2009. Soluble epoxide hydrolase as a therapeutic target for cardiovascular diseases. *Nat. Rev. Drug Discov.* **8:** 794–805.
46. Perl, E. R. 2007. Ideas about pain, a historical view. *Nat. Rev. Neurosci.* **8:** 71–80.
47. Smith, W. 1989. Eicosanoid nomenclature. *Prostaglandins.* **38:** 125–133.